International Journal of Heat and Fluid Flow 73 (2018) 223–235

Contents lists available at ScienceDirect

International Journal of Heat and Fluid Flow

journal homepage: www.elsevier.com/locate/ijhff

The role of surface texturing on the physics of boundary layer separation over a bump☆

N. Beratlis*,[a], E. Balaras[b], K. Squires[a]

[a] Department of Mechanical Engineering, Arizona State University, Tempe, AZ 12345, USA
[b] Department of Aerospace and Mechanical Engineering, The George Washington University, Washington, DC 20052, USA

ARTICLE INFO

Keywords:
Flow separation
Surface texturing
Drag reduction

ABSTRACT

In the present work the effects of different types of roughness elements on flow separation over a circular bump is investigated by means of direct numerical simulations. Two types of roughness elements are considered, dimples and spherical beads. The boundary condition setup and the Reynolds number range were selected to replicate in a qualitative sense the initial development of the boundary layer (growth, transition, separation) on full cylinders or spheres, which is primarily responsible for the trends in the behavior of their drag coefficient. Both roughness elements are very effective in causing transition of the boundary layer at a much lower Reynolds number when compared to a smooth surface. For the spherical beads the drag coefficient exhibits a minimum and quickly rises as the Reynolds number increases. For the dimples the minimum drag coefficient remains constant and independent on the Reynolds number within the range considered in this study. This behaviour agrees with experimental observations in the literature for similar types of roughness elements. The differences are due to the way the boundary layer grows over dimples or spherical beads. For the latter, transition shifts upstream and moves toward the stagnation point on the front of the body as the Reynolds number increases. An earlier transition means the boundary layer starts growing thicker earlier and has less momentum to overcome the adverse pressure gradient. As a result the separation point moves upstream too giving rise to increased drag. In contrast the transition and separation points are weakly dependent on the Reynolds number for the case of the dimples.

1. Introduction

Various roughness elements have been used to reduce the drag force on both bluff and streamlined bodies. Fig. 1 shows the variation of the drag coefficient, C_D, versus the Reynolds number, $Re = UD/\nu$, (where U is the free-stream velocity, D is the diameter of the sphere and ν is the kinematic viscosity), for spheres with smooth or roughened surfaces compiled from different experiments in the literature (Achenbach, 1974; Bearman and Harvey, 1976; Choi et al., 2006). For the smooth sphere the drag coefficient drops sharply to its lowest value of $C_D = 0.08$ when the Reynolds number is $Re \sim 400,000$, and starts to augment as the Reynolds number increases. The decrease in C_D can be directly linked to the state of the boundary layers on the sphere, which transition from laminar to turbulent. This phenomenon is typically termed the *drag-crisis* taking place at the *critical* Reynolds number. The flow regimes for Reynolds numbers lower and higher than the critical value are called *sub-critical*, and *post-critical* respectively. The boundary layer on the sphere is laminar for the former and turbulent for the latter. When roughness elements are used the drag-crisis can be shifted at lower Reynolds numbers, lowering the drag coefficient compared to that of a smooth sphere at the same Reynolds number.

The type of roughness element plays an important role in this process. Achenbach (1974) conducted experiments on spheres roughened with small glass beads directly glued to its surface or using sandpaper. In all cases, as the size of the roughness elements increases the critical Reynolds number is reduced. However the minimum drag coefficient is not maintained over a broad Reynolds number range and rises quickly in the post-critical regime (see Fig. 1). Wind tunnel experiments on cylinders with sandpaper wrapped around their perimeter Güven et al. (1980) and Achenbach (1971), reported similar behavior for the drag coefficient. It was conjectured that for this type of roughness (sand-grain), increasing the Reynolds number in the post-critical regime results in shifting the transition point upstream generating a turbulent boundary layer that thickens faster and separates earlier increasing the drag coefficient.

☆ Fully documented templates are available in the elsarticle package on CTAN.

* Corresponding author.
E-mail address: nikos.beratlist@gmail.com (N. Beratlis).

https://doi.org/10.1016/j.ijheatfluidflow.2018.08.006
Received 5 December 2017; Received in revised form 23 August 2018; Accepted 24 August 2018

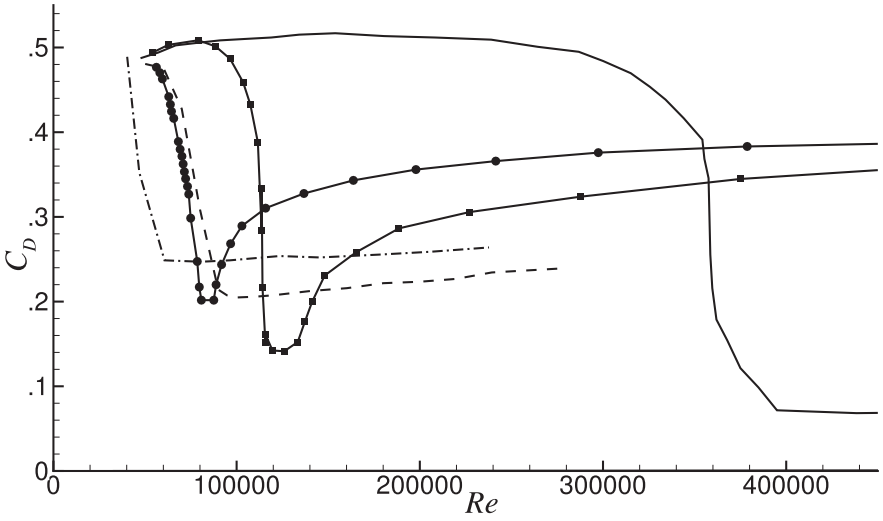

Fig. 1. Plot of drag coefficient C_D versus Reynolds number for a stationary smooth sphere, various golf balls and spheres with sand-grain roughness. Lines represent: —; smooth sphere (Achenbach, 1974) , - - -; dimpled sphere $k/D = 4 \times 10^{-3}$ (Choi et al., 2006), - · -; dimpled sphere $k/D = 9 \times 10^{-3}$ (Bearman and Harvey, 1976), -■-; rough sphere $k/D = 0.5 \times 10^{-3}$ (Achenbach, 1974), -•-; rough sphere $k/D = 1.25 \times 10^{-3}$ (Achenbach, 1974).

In Fig. 1 the variation of C_D vs Re is also shown for dimpled spheres (data from the experiments in Bearman and Harvey, 1976; Choi et al., 2006), where a very different behaviour is observed. Contrary to sand-grain roughness, dimples can maintain the low drag coefficient over a wide range of Reynolds numbers in the post-critical regime. The origin of this behaviour however is not well understood. Choi et al. (2006) carried out some of the most detailed wind tunnel experiments on dimpled spheres, measuring velocities within the dimples. They observed that dimples cause local flow separation leading to the formation of a detached shear layer, which then become unstable and generates vortical structures, leading to the formation of a turbulent boundary layer. They also reported that the transition location was not very sensitive to the Reynolds number, which may be responsible for the insensitivity of C_D to the Reynolds number in the post-critical regime. Dimple type (i.e. hexagonal or spherical) and size affect the critical Reynolds number and the minimum value of C_D in the post-critical regime, but the lack of sensitivity to Reynolds number appears to be fairly robust. Aoki et al. (2012) conducted experiments with dimpled spheres varying systematically the depth of the dimples. They found that as the dimple depth increased the critical Reynolds number decreased, and the separation point shifted upstream giving higher drag in the post-critical regime. Aoki et al. (2003) also examined the effects of dimple coverage, by measuring the drag forces on spheres with different numbers of the same size dimples. They showed that as the number of dimples increased the critical Reynolds number decreased and the minimum drag coefficient increased.

From the above review it is clear that roughness elements accelerate the transition of the laminar boundary layer on a bluff body decreasing the critical Reynolds number. As a result the drag coefficient when compared to that of the smooth body at the same Reynolds number is substantially decreased. This is true for large-scale elements, such as dimples, which have a diameter 10–20 times the thickness of the incoming laminar boundary layer, as well as smaller elements which are a small fraction of the incoming boundary layer. The evolution of the drag coefficient vs Reynolds number in the post-critical regime, however, is very different for the above classes of roughness elements, and the underlying mechanics are not well understood. In most studies of dimpled spheres and cylinders, for example, the drag coefficient remains constant in the post-critical regime while for the case of sand-grain roughness it rapidly increases as a function of the Reynolds number.

The primary objective of the present study is to better understand the origin of this behaviour using Direct Numerical Simulations (DNS). Most likely the growth/evolution of the turbulent boundary layer over the roughness elements, which is generated as a result of their interaction with the incoming laminar boundary layer, is very different for different elements. Beratlis et al. (2014) studied the evolution of a boundary layer with zero pressure gradient over a flat plate covered with dimples of the same size. They conducted DNS and varied the numbers of rows of dimples encountered by the incoming flow. It was shown that the shear layer that forms over the first row of dimples becomes unstable and rolls up into a coherent vortex sheet, that transforms itself into packets of Λ-type vortices reorienting the spanwise vorticity into streamwise. These vortices evolve further and populate the turbulent boundary layer. This is in qualitative agreement with the measurements within dimples on the surface of a golf-ball conducted by Choi et al. (2006). When multiple rows of dimples were used, the mixing across the boundary layer was enhanced, resulting in thickening and momentum transfer away from the wall. Beratlis et al. (2016) used a similar flat-plate configuration to study the effects of different types of roughness elements (circular groove, circular dimple, and hexagonal dimple) on the flow. They found that the type of element plays an important role in the transition mechanism, as well as the evolution of the boundary layer downstream. It was shown that the primary effect of the dimple geometry on the boundary layer is to cause a distinct shift in the virtual origin of the boundary layer. Velocity profiles when compared at the same downstream location exhibit important momentum deficits away from the wall for the three different geometries. However, when the shift is accounted for by plotting quantities at the same Re_θ, the statistics collapse and agree well with those of a canonical turbulent boundary layer with zero pressure gradient.

The above studies provide a detailed view of the interaction of boundary layers with large elements such as dimples, but could not be directly used to interpret the behaviour of C_D vs Re_D in Fig. 1, as they do not account for the effects of curvature and strong pressure gradients present for the case of flow around spheres. In addition, sand-grain type elements were not considered. In the present work we used existing experimental results as a guide, and targeted specific configurations to be able to identify the physics behind the trends observed in Fig. 1. For example, the case of a dimpled sphere with dimple depth, $d = 4 \times 10^{-3}D$, and a sphere covered with spherical beads of diameter $b = 0.5 \times 10^{-3}D$ have very similar critical Reynolds numbers ($Re_D \sim 90,000$), and a minimum drag coefficient $C_D \sim 0.2$. The dimple depth and dimple diameter on the other hand, are one and two orders of magnitude larger than the bead size respectively. For the dimpled sphere the